Detrimental contribution of the immuno-inhibitor b7-h1 to rabies virus encephalitis.

Monique Lafon, Françoise Mégret, Sven G Meuth, Ole Simon, Myriam L Velandia Romero, Mireille Lafage, Lieping Chen, Lena Alexopoulou, Richard A Flavell, Christophe Prehaud, et al.

Detrimental contribution of the immuno-inhibitor B7-H1 to rabies virus encephalitis

Monique Lafon [*†], Françoise Mégret[†], Sven G Meuth [‡], Ole Simon [‡], Myriam Lucia Velandia Romero[†,§], Mireille Lafage[†], Lieping Chen[¶], Lena Alexopoulou[ll], Richard A Flavell[#], Christophe Prehaud[†] and Heinz Wiendl [‡]

[†]Viral Neuroimmunology, Institut Pasteur, Paris, France

[‡]Department of Neurology, Julius-Maximilians-University of Wuerzburg, Wuerzburg, Germany

[§]Instituto de Virologia, Universitad El Bosque, Bogota, Colombia

[¶]Department of Dermatology and Oncology, Johns Hopkins University School of Medicine, Baltimore, Maryland, USA

[ll] Centre d'Immunologie de Marseille-Luminy, Marseille, France

[#] Section of Immunobiology, Yale University School of Medicine, New Haven, USA

Running title : B7-H1 mediated rabies immunosubversion

* Corresponding author: Monique Lafon, Laboratoire de Neuroimmunologie Virale, Institut Pasteur, 25, rue du Dr Roux, 75724 Paris Cedex 15, France,
tel: 33 1 45 68 87 52, fax: 33 1 40 61 33 12. e-mail: mlafon@pasteur.fr

Key words : B7-H1, PD-L1, B7-DC, TLR3, neurons, rabies virus, IFN-β

This work was supported by grants from Institut Pasteur including PTR 186 (to M.L.), the Deutsche Forschungsgemeinschaft (SFB581, TPA8 to H.W.) and the IZKF (Interdisciplinary Center for Clinical research, 48-0-0, to H.W.).

Abstract

Rabies virus is the etiological agent of an acute encephalitis, which in absence of post exposure treatment is fatal in almost all cases. Virus lethality rests on its ability to evade the immune response. Here, we analyzed the role of the immuno-inhibitory molecule B7-H1 in this virus strategy. We showed that in the brain and spinal cord of mice, rabies virus infection resulted in significant up-regulation of B7-H1 expression, which is specifically expressed in infected neurons. Correlatively, clinical rabies in B7-H1$^{-/-}$mice is markedly less severe than in wild type mice. B7-H1$^{-/-}$mice display resistance to rabies. Virus invasion is reduced and the level of migratory CD8 T cells increases into the nervous system, while CD4/CD8 ratio remains unchanged in the periphery. *In vivo*, neuronal B7-H1 expression is critically depending on TLR3 signalling and IFN-β, since TLR3$^{-/-}$ mice - in which IFN-β production is reduced - showed only a limited increase of B7-H1 transcripts after infection. These data provide evidence that neurons can express the B7-H1 molecule after viral stress or exposure to a particular cytokine environment. They show that the B7-H1/PD-1 pathway can be exploited locally and in an organ specific manner - here the nervous system - by a neurotropic virus to promote successful host invasion.

Introduction

Rabies remains an important public health problem in the world due to uncontrolled enzootic rabies, lack of vaccines and poor information on the risk of contracting rabies after animal exposure. Globally there are over 70 000 cases of rabies reported each year. Rabies is now a re-emerging disease in several parts of the world including China where epidemics are currently exploding. Rabies virus (RABV), which is transmitted by bites of rabid animals, replicates in nervous tissues - only in neurons -, causing fatal encephalitis in nearly every case (1). In the absence of post-exposure treatment, rabies is one of the very few human infections reaching a nearly 100 % mortality rate (2). Recently, a spectacular and fortunate case of survival in the absence of rabies prophylaxis was reported (3). Rabies recovery after obvious infection of the nervous system (NS) provides new hope that the striking evasive strategies of RABV (4, 5) can in some instances - and so far for unknown reasons - be disarmed. This urges us to investigate in depth how RABV infection modified human neuron physiology. It has been proposed that upregulation of immunoevasive molecules may contribute to the RABV strategy (6, 7). Using an *in silico* analysis of the transcriptome of RABV infected human neurons, we managed to identify the co-inhibitor B7-H1 as a putative target of RABV to escape the host immune response.

T cell activation generally incorporates self-limiting mechanisms, such as inhibitory stimulation, to regulate T cell tolerance and attenuate the immune response. PD-1 (Programmed death 1) is one member of the inhibitory molecules belonging to the B7-CD28 which provide inhibitory functions to B and T cells. PD-1 expressed on T and B cells has two ligands, B7-H1 (alternatively programmed cell death ligand 1, PD-L1) and B7-DC (alternatively programmed cell death ligand 2, PD-L2). Ligation of PD-1 by B7-H1 inhibits T cell proliferation and cytokine production, leading to immunological tolerance in different immune compartments (8-13). B7-H1 is expressed under the control of IFN-γ (14) and IFN-

β (12). It is found on lymphoid tissues as well as in a variety of non-lymphoid tissues such as muscle, microvascular endothelial, renal tubular cells, ocular cells and in cancer cell lines (11, 14-20). In the inflamed NS, microglia and macrophages were identified as the main sources of B7-H1 expression (11, 21).

Ectopic expression of immune inhibitory B7-H1 by tumors serves as a mechanism for immune evasion (18, 22). Viruses that specifically induce expression of B7-H1 or B7-DC in infected cells may down regulate the host immune response and favour infectiveness (19, 23). Blockade of the PD-1 pathway may augment antimicrobial immunity and diminish persistent infection in mice. This may lead to new ways of treating chronic viral infections in humans (8, 24). Manipulation of the B7-H1/PD-1 pathway alters the course and severity of autoimmune NS inflammation in animal models of experimental allergic encephalomyelitis (21, 25, 26).

Although B7-H1 is virtually absent from the non-infected NS (4, 7), we wondered whether modulation of B7-H1 could be employed by RABV to escape adverse host immune responses. We therefore investigated 1) whether B7-H1 was modulated in the NS of mice infected with RABV, 2) whether RABV-infected neurons express B7-H1 and 3) by using B7-H1$^{-/-}$ mice, whether the B7-H1 pathway contributes to RABV neuroinvasiveness.

MATERIALS AND METHODS

Ab and reagents

Biotinylated anti-mouse B7-H1 (clone MIH5) and biotinylated anti-human B7-H1 (clone MIH1) were from eBioscience. Anti human B7-H1 NH2 terminus (H-130) Ab was from Santa cruz Biotechnology. MAP 2 a/b specific Ab was purchased from Abcam. FITC-conjugated rabbit anti-RABV nucleocapsid Ab was from BioRad. Alexa Fluor594-conjugated streptavidin was purchased from Molecular Probes. Cy5-conjugated donkey anti-rat IgG was from Jackson Immuno Research. Fluoromount-G was obtained from Southern Biotechnology Associates. Fc-Block (anti Fcγ III/II receptor rat mAb), anti mouse CD3, CD19, CD8 and CD4 antibodies were from BD Biosciences. Hot Start Taq polymerase and RNeasy Protect kit and Lipid Tissue Midi Kit were purchased from Qiagen. Superscript II RT was from InVitroGene. RNA Nano Chips were obtained from Agilent Technologies. Recombinant human IFN-β was from Schering, rTNF−α, from Pharmingen and rIFN-γ from R&D. Percoll was from Amersham Biosciences. OCT compound was from Miles.

Virus, human neural cells and mice

The laboratory RABV strain CVS (ATCC vr959), a highly pathogenic RABV strain (27) causing fatal encephalomyelitis in mice, was propagated as described (28). HSV-1 strain KOS (29) was propagated on U373MG. B7-H1$^{-/-}$ and TLR3$^{-/-}$ mice were generated as described (30, 31). Six-week-old C57Bl6 from Janvier (St. Berthevin, France), B7-H1$^{-/-}$ or TLR-3$^{-/-}$ female mice were inoculated intramuscularly in both hind legs, with $1x10^7$ infectious particles of RABV. Disease progression was evaluated as described by scoring clinical signs and mortality (6). Mobility and mortality were scored as follows: 0 = normal mice, 1 = ruffled fur, 2 = one paralysed hind leg, 3 = two paralysed hind legs, 4 = total paralysis (defined as the total loss of mobility) and 5 = death. Daily clinical score was obtained by adding individual

scores. Dead mice were reported in the clinical score of the day of the death and thereafter (cumulative scores). Disease progression was presented by a curve of cumulative clinical scores. At days 5, 7 and 9 after infection, groups of two or three mice were perfused. Spinal cords and brains were removed separately and stored at –80°C before being processed for RNA extraction, immunohistochemistry or mononuclear cell isolation by percol gradient. Animal housing and experimental protocols followed guidelines approved by French Ministry of Agriculture and Ethical committee.

Human NT2-N neurons (32) and mixed cultures neurons/astrocytes, NT2-N/A (33) were differentiated from Ntera-2clD/1 cells as described (34, 35). Purity of the NT2-N and mixed composition of NT2-N/A were checked by RT PCR as described (36). Human neuroblastoma SK-N-SH cell lines (ATCC: HTB, cat N°11), SK-N-SH-CP, a natural mutant of SK-N-SH disabled for expression of IFN-β, NT2-N and NT2-N/A cultures were infected with RABV or HSV-1(7, 36) or treated for 24h and 48h with IFN-β (1000 U), IFN–γ (500 U) or TNF–α (1.25ng) when needed. Infection was detected by RT-PCR using primers directed against the HSV-1 UL54 gene or the RABV N gene amplicons and by immunocytochemistry as described (37).

Cell cultures from mouse hippocampi prepared from embryos (C57Bl/6 mice) at stage E 18 as previously described (11) were incubated with cytokines (IFN-γ and-β 500 U/ml and 1000 U/ml, respectively) for 48h.

Standard and real time RT-PCR

Total RNA was extracted with RNeasy kit (for cells) 24h after infection or cytokine treatment, or with Lipid Tissue MidiKit (for nervous tissues). RNA quality was monitored using Agilent RNA chips. cDNA synthesis was performed with oligodT primers (**Table 1**). Real-time PCR was performed as described (11). Values were expressed as relative increase compared to

normalized non-infected or non-treated control (value set to 1) according to the manufacturer's instructions.

Immunohistochemistry and immunocytochemistry

Dissected brains and spinal cords were snap frozen and embedded in tissue-Tek OCT. Cryostat sections (8µm) were fixed in 4% Paraformaldehyde (PFA), permeabilized in SPB-0,5% Triton X-100, incubated with blocking buffer (5% goat serum and 2% BSA in SPB) and treated 1h at room temperature (Rt) with biotinylated anti-B7-H1 mouse mAb, then by Alexa Fluor 594-conjugated streptavidin for 30 min at Rt as well as with a rabbit polyclonal FITC-conjugated Ab directed against RABV nucleocapsid.

Immunochemistry on hippocampus cultures was performed on 7 day cultured cells fixed in 20% PFA and blocked with 10 mM SPB, 10% horse serum, 0.2% Triton X100. Slides were incubated 1h at Rt with rat anti-mouse B7H1 and anti-MAP2 a/b mouse Ab then with Cy5-conjugated donkey anti-rat IgG and Cy-2 conjugated donkey anti mouse finally with DAPI. Coverslips were mounted in Fluoromount-G and the samples observed under a Leica DM 5000B UV. Images were processed with the Leica FW 4000 software.

Cytofluorimetry for B7-H1 surface expression

Surface expression of B7-H1 was analyzed by flow cytometry. Gently scraped off infected and non-infected SK-N-SH were incubated with biotinylated B7-H1 specific mAb (clone MIH1, 2µg/10^6 cells) and then with FITC-conjugated streptavidin. Cells were analyzed by flow cytometry, using a BD Biosciences FACScalibur equipped with Cell Quest Pro software. Specific fluorescence indices (SFIs) greater than 1.25 were considered positive.

Phenotyping of splenocytes and mononuclear cells infiltrating the NS

CNS mononuclear cells were collected from homogenates of brain and spinal cord samples onto percoll gradients as described (37). Splenocytes or mononuclear cells infiltrating the NS (10^5 in 50µl) were assessed by flow-cytometry using predetermined optimal concentrations of fluorescent pairs of mAb (CD3/CD19, CD4/CD3 and CD8/CD3). Data analysis was performed with Cell Quest Pro.

Measurement of T cells apoptosis in brain infiltrating T cells.

Morphological changes to identify cell in intermediate / late stages of apoptosis were assayed by side (SSC) and forward light scattering (FSC) flow cytometry analysis as previously described for T cells (38, 39).

RESULTS

Activation of B7-H1 mRNA and protein expression by RABV in human neurons

Previous transcriptome analysis of RABV infected human neurons NT2-N, has allowed us to identify the co-inhibitor B7-H1 as a putative target of RABV to escape the host immune response. Further analysis of the neuronal expression of B7-H1 upon RABV infection was pursued in cell cultures of human NT2-N and in a human neuroblastoma cell line (SK-N-SH). NT2-N cell cultures are nearly pure populations of terminally differentiated post-mitotic cells. They display biochemical, morphological and functional characteristics of human neurons (40, 41). Control experiments were performed on the same cells infected with HSV-1. Kinetics of B7-H1 transcription in NT2-N after 1, 6 and 24h post RABV infection were followed by real time PCR and compared to non-infected conditions (**Figure 1A**). The yield of *B7-H1* mRNA transcription (black histogram) became detectable after 6h of RABV infection and markedly increased as infection progressed (grey histograms). B7-H1 molecules could also be detected by cytofluorimetry on the surface of RABV-infected SK-N-SH neuroblastoma after 24h of infection (**Figure 1B)**. This evidence was obtained with two distinct B7-H1 Ab from two different sources. This means B7-H1 molecules have reached a location where they could potentially interact with their receptors. As a control experiment, NT2-N cells were infected with HSV-1 under the same experimental protocol as above. Despite a strong infection, as evidenced by RT-PCR (**Figure 1A, right panel**) and immunocytochemistry (data not shown), no significant increase of *B7-H1* mRNAs could be observed (**Figure 1A,** HSV-1 24h). B7-H1 up-regulation in human neurons seems therefore specific of RABV infection.

Regulation of other B7-ligands after RABV infection in human neuronal cultures and in mixed astroglial/neuronal cultures

The neuronal expression of other members of the B7-family could be affected by RABV infection. We compared the expression level of *B7-DC* (PD-L2), *B7.1* (CD80) and *B7.2* (CD86) mRNA after RABV infection in NT2-N and in non-infected cells (**Figure 1C**). RABV led to a modest increase of *B7-DC* (2fold, black histogram) compared to non-infected cells (white histogram), whereas *CD80* and *CD86* transcripts were virtually unmodified since the level of transcription was similar to those of *CD200R* used as negative controls. In addition, the putative contribution of astrocytes to *B7-H1* expression in the NS was analyzed in mixed cultures of human neurons and astrocytes (NT2-N/A). The mixed culture mimics the physiological conditions of NS infection by this virus *in vivo*, as RABV primarily infects neurons and not astrocytes (7, 42). As observed in NT2-N, RABV infection induced up-regulated mRNA expression of *B7-H1* and *B7-DC* transcripts in NT2-N/A in a similar manner as those observed in NT2-N (data not shown), suggesting that neurons mainly contribute to *B7-H1* mRNA expression. Neither *B7-DC* nor *B7-H1* transcription were up-regulated in NT2-N or NT2-N/A after HSV-1 infection (**Figure 1C**, grey histograms) indicating that up-regulation of *B7-H1* and *B7-DC* - the two ligands of PD-1 - is RABV specific.

In the absence of infection, IFN-β, or –γ trigger B7-H1 expression in human and mouse neural cell cultures

During the course of infection of NT2-N cultures by RABV, expression of B7-H1 mRNA appeared to correlate well with the development of the viral load (compare the two histograms in **Figure 1A**). IFN-ß mRNA monitored under the same conditions of infection followed a different time course. IFN-β transcription presented a 16-fold increase as early as 1h post infection and peaked at 6h post infection (3 x10^4 increase; data not shown). It clearly

preceded the induction of B7-H1 mRNA synthesis. In contrast, HSV-1 infection did not trigger *B7-H1* expression and did not induce *IFN-β* expression either (data not shown and (36)). IFN-β might therefore be required for the induction of B7-H1 expression. We therefore analyzed whether the addition of IFN-β to non-infected human NT2-N and NT2-N/A triggers *B7-H1* expression. Addition of IFN-γ and TNF-α was tested in parallel. IFN-β-treatment (24h, 1000U) led to a significant up-regulation of *B7-H1* transcription in NT2-N (appr.50 fold; data not shown) and in NT2-N/A (150 fold; **Figure 1D,** black histogram), therefore indicating that exogenous IFN-β can trigger *B7-H1* expression in human neurons and co-cultures of neurons and astrocytes. Addition of IFN-γ also caused an 80-fold increase of the expression of B7-H1 transcripts in NT2-N/A, whereas TNF–α has a limited effect **(Figure 1D**). Of note, B7-DC transcription was only triggered to very limited amounts by IFN–γ, β and TNF–α in human neurons/astrocytes cultures (**Figure 1D,** grey histogram).

Notably, B7-H1 protein expression was also up-regulated in cultures of mouse hippocampus neurons exposed to IFN–γ or –β for 48 h (**Figure 2**).

In the absence of IFN-β expression , RABV does not trigger B7-H1 expression in human neural cell cultures

To test whether in the absence of IFN-β, RABV can still upregulate B7-H1 expression, we used a human neuroblastoma cell line naturally disabled in the IFN expression (SK-N-SH-CP). We observed in these cells that in absence of IFN-β signalling, RABV cannot upregulate B7-H1 expression anymore (**Figure 1E**), supporting strongly the role of IFN-β in the control of B7-H1.

Expression and regulation of B7-H1 in the mouse NS after RABV infection

First, we monitored the expression and regulation of B7-H1 during NS infection by RABV by assessing brain and spinal cord specimens from animals at an early (day 5) and a late stage of infection (day 7) using real time RT-PCR as well as immunohistochemistry. As expected (11), *B7-H1* mRNAs were virtually undetectable in the non-infected NS. In contrast, *B7-H1* mRNA expression progressively increased during the course of infection and correlated with the invasion of spinal cord and brain by the virus (**Figure 3A**). In order to identify the cellular source of B7-H1, we performed double immuno-staining analysis detecting infected neurons (in green) and B7-H1 (in red) in brain specimens at days 5 and 7. As shown in **Figure 3B (x and y axis) and C (x and y axis and orthogonal analyses)** infected neurons can express B7-H1 (**upper panel**). This expression occurs primarily in the cellular bodies of RABV infected neurons and not in the neurites (**lower panel of 3B**). The vast majority of infected neurons (70%) can express B7-H1. B7-H1 was also expressed by non-infected cells (data not shown) which correspond to endothelial cells, $GFAP^+$ astrocytes, $CD11b^+$ monocyte/macrophages and migratory $CD3^+$ T cells (11, 21). The B7-H1 positive $CD3^+$ T cells appeared only at late stages of infection (day 7).

IFN–β rather than IFN–γ is a key cytokine contributing to B7-H1 up-regulation in RABV infected NS

After having demonstrated the expression of B7-H1 after RABV infection in neuronal cells *in vivo* and *in vitro*, we next questioned which cytokines or cytokine-inducing pathways were involved in this *in vivo* up-regulation. Experiments in WT mice showed that IFN–β and –γ expression in the CNS of infected mice (**Figure 4A**) was concomitant with an increase of *B7-H1* expression (see **Figure 3A**). To further analyse the role of IFN-β in the up-regulation of B7-H1 after RABV-infection, we investigated mice with impaired IFN-β production. As a

model, we initially used mice lacking receptor for IFNα/β (IFN-Rα/β$^{-/-}$ mice). However, in these mice rabies is fulminant. All mice were dead 4 days after infection, a period too short to study *B7-H1* up-regulation in the brain (data not shown). We turned to TLR3$^{-/-}$mice (31) because we noticed that upon RABV infection, *IFN-β* expression was significantly decreased in TLR3$^{-/-}$mice brains compared to wild type (WT) mice. TLR3$^{-/-}$ and WT mice were infected with RABV and sacrificed 5 and 7 days after infection. Transcripts of *IFN-β,-γ* and *B7-H1* were quantified in the brain by real-time PCR (**Figure 4B**). We found that *B7-H1* up-regulation at day 7 was significantly decreased in TLR3$^{-/-}$ mice brains in comparison to WT (152 fold increase in WT and 56 fold increase in TLR3$^{-/-}$ brains). This was concomitant with a limited up-regulation of *IFN-β* mRNA as compared to WT (516 fold increase in WT compared to 113 fold increase in TLR3$^{-/-}$ mice). In contrast, *IFN-γ* up-regulation was not reduced but showed a significant increase (7-fold increase compared to *IFN-γ* transcription in WT brains). However, despite the high expression of IFN-γ transcripts in TLR3$^{-/-}$ mice, *B7-H1* expression was diminished. These observations support the hypothesis that IFN-β - and not IFN-γ – is a key contributor to the up-regulation of B7-H1 expression in the NS upon RABV infection.

Contribution of B7-H1 to immune evasion in RABV infection

We found that RABV specifically triggers the regulation and the surface expression of B7-H1 in infected neurons. Various reports have demonstrated that B7-H1 provides an inhibitory signal in the interaction with antigen-specific T-cells. Importantly, B7-H1 is responsible for the exhaustion of antiviral T cell responses by triggering the anergy of activated T cells (19). We therefore tested whether this key molecule was involved in the immunoevasive strategy of RABV. To do so, we compared the progression and the outcome of RABV infection in mice lacking B7-H1(30) with WT mice. B7-H1$^{-/-}$ mice and control WT C57Bl6 mice (n=8 in each

group) were injected with a dose of virus expected to kill half of the mice (ED50). Mice were observed during 16 days post infection. Progression of the disease in the two groups of mice is illustrated by the cumulative clinical curves. Clinical signs (**Figure 5A**) as well as mortality records (**Figure 5B**) were assessed. In both groups, half of the mice started losing weight 6 days after infection (data not shown) indicating that they were infected. Consistent with our expectation for this injected dose, in both groups, half of the mice showed clinical signs of disease including loss of hindlimbs mobility. However, in striking contrast to disease course observed in WT animals, clinical signs of encephalitis such as hunchback did not occur in sick B7-H1$^{-/-}$ mice. Mean cumulative clinical score was significantly decreased in B7-H1$^{-/-}$ mice compared to WT mice (**Figure 5A**). By day 9, consistent with the dose of virus injected (dose 50), half of the WT mice died, whereas B7-H1 mice survived (**Figure 5B)**. Infection of mice with a dose which killed 100 % of WT mice (dose 100) only killed half of the B7-H1 mice (**Figure 5B**). Neuroinvasiveness was compared in those mice, by measuring the amount of transcripts of viral N protein in the brain stem of RABV-infected WT and B7-H1$^{-/-}$mice at days 5 and 10. A reference value of 1, taken for non-infected NS, was used for calibration. As shown in **Figure 5C**, the viral transcription was drastically reduced in B7-H1$^{-/-}$ NS (38 fold less) as early as day 5 (83 value for N mRNAs in B7-H1$^{-/-}$ and 3.200 in WT NS samples). The difference was more pronounced at day 10 post infection, with 690-fold less viral transcription in the brain stem of B7-H1$^{-/-}$ mice than in WT (460-fold increase of N mRNAs for B7-H1$^{-/-}$ and 320 000 fold increase in WT mice). RABV neuroinvasiveness was therefore severely impaired in the absence of B7-H1.

RABV was also less severe in TLR3$^{-/-}$ mice than in WT mice (mortality was reduced by a two-fold factor, 63% mortality in WT versus 34% mortality in TLR3$^{-/-}$ mice; data not shown). Of note, as shown in **Figure 4,** *B7-H1* was less transcribed in neural tissues of RABV infected TLR3$^{-/-}$ mice than in WT mice.

$CD8^+$ T cell infiltration into the RABV infected NS is maintained in the absence of B7-H1

We previously observed that the severity of RABV infection was inversely correlated with the number of $CD3^+$ and $CD8^+$ T cells in the NS (6, 37). Conclusions of these previous studies were that highly neuroinvasive and pathogenic infections were associated with a severe drop in the number of $CD3^+$ T cells of migratory cells into the NS, whereas high amounts of $CD3^+$ or $CD8^+$ migratory T cells were observed in poorly neuroinvasive and less pathogenic RABV infection.

The effect of RABV infection on the subpopulations of $CD3^+$, $CD4^+$ and $CD8^+$ in the pool of migratory T cells into the NS was further analysed by cytofluorimetry and compared to those found in the periphery (spleen). WT and B7-$H1^{-/-}$ mice were infected with RABV. Splenocytes and NS immune cells were analyzed by cytofluorimetry 5 and 10 days post-infection in WT and B7-$H1^{-/-}$mice. Analysis of $CD4^+$ and $CD8^+$ splenocytes indicated that RABV infection does not modify the CD4/CD8 ratio in the spleen during infection of WT and B7-$H1^{-/-}$ mice (**Table 2**).

The nature of the cells invading the NS and the time course of the invasion were compared in the two groups of mice. Five days after RABV infection, and in contrast to what was observed in the absence of infection, mononuclear cells started to invade the infected NS (**Figure 6A**). Invasion of $CD3^+$ T cells was observed already at day 5. No difference was found between WT and B7-$H1^{-/-}$ mice ($CD3^+$ T cells represented 55% of the migratory cells in WT and 62% in B7-$H1^{-/-}$ NS). As described previously (6), the pool of migratory $CD3^+$ T cells in the WT NS dropped later (here at day 10 post infection; **Figure 6A**). This decrease of $CD3^+$ T cells was mainly due to a drastic disappearance of $CD8^+$ T cells ($CD8^+$ T cells represents only 3% of the $CD3^+$ T cells migratory pool), whereas the pool of $CD4^+$ T cells is more stable (**Figure**

6B and 6C). The drop of $CD8^+$ T cells might account for the increase of the CD4/CD8 ratio which rises from 2.9 at day 5 up to 5.8 at day 10 (**Figure 6D**). In striking contrast to WT mice, neither the decrease of $CD3^+$ T cell at day 10, nor the $CD8^+$ T cell decrease were observed in infected B7-$H1^{-/-}$ mice (**Figure 6A and B**). At day 10, $CD8^+$ T cells still account for 20% of $CD3^+$ T cells in infected B7-$H1^{-/-}$mice (compared to only 3% in RABV infected WT mice, **Figure 6C**). As a consequence, the CD4/CD8 ratio remained stable at day 10 post infection in the NS of B7-$H1^{-/-}$ mice (**Figure 6D**). Apoptosis of migratory T cells in the brain of RABV infected B7-$H1^{-/-}$ and WT mice was analyzed 5 days post infection by cytofluorimetry analysis taking reduction in size and increase of granulometry as a marker of T cell apoptosis as described (38) (**Figure 6E**). 5 days after infection whereas 70% of migratory $CD8^+$T cells in WT mice were engaged in an apoptotic process, this percentage was reduced by 50% in the absence of B7-H1, indicating that, $CD8^+$ T cells are partially protected against RABV mediated apoptosis in the absence of B7-H1.

Therefore, the absence of B7-H1 correlated with the preservation of high amounts of CD3/CD8 migratory T cells and with a significant reduction of the viral invasiveness. These findings strongly suggest that up-regulation of B7-H1 taking place in infected neurons and in a WT context contributes to the exhaustion or eradication of $CD8^+$ T cells and thus favors the escape of virus infection from the host immune response.

Discussion

Our report identifies an important and new role of the co-inhibitory B7-H1 pathway in antiviral NS immunity. Upon viral infection with RABV, B7-H1 expression was found to be up-regulated in NS cells including neurons. Mice lacking a functional *B7-H1* gene, B7-H1$^{-/-}$ mice displayed a marked resistance to rabies. Resistance to viral infection in B7-H1$^{-/-}$ mice was associated with a reduced viral load in the NS and with an increase of infiltrating CD8^{+} T cells into the NS, whereas immune response in the periphery was not different from WT mice.

RABV is a pathogen well-adapted to the NS, where it infects neurons. It is transmitted by the bite of an infected animal. It enters the NS via a motor neuron through the neuromuscular junction, or via a sensory nerve through nerve spindles. It then travels from one neuron to the next, along the spinal cord to the brain and the salivary glands. The virions are excreted in the saliva of the animal and can be transmitted to another host by bite (43). Thus, preservation of the neuronal network integrity is crucial for the virus. Successful invasion of the NS by RABV seems to be the result of a subversive strategy based on the survival of infected neurons (5, 44). This strategy includes protection against virus-mediated apoptosis and destruction of T and NK cells that invade the NS by redundant control of the expression of the immunosubversive molecules FasL and HLA-G (4, 6, 44). The present study strongly suggests that this strategy also includes CD8^{+} T cell exhaustion/death by the B7-H1/PD-1 pathway. CNS-derived B7-H1 might be operative in inhibiting local T cell expansion or even directly “eliminate” T-cells, e.g. by apoptosis (6) as demonstrated in other systems, such as cornea (20). Previous studies indicated that T cells entering the NS underwent apoptosis in the course of RABV infection in mice (5, 6). We observed that in WT mice, the CD8^{+}T cells entering the NS encounter apoptosis (**Figure 6E**), this number was reduced by 50% in the B7-H1$^{-/-}$ mice, indicating that B7-H1 contributes to the apoptosis of effector T cells infiltrating

the infected NS. B7-H1 mediated killing of $CD8^+$ T cells was obtained in co-cultures of MHC and B7-H1 expressing neurons with activated OT-1 $CD8^+$ T cells (SM, OS and HW manuscript in preparation). The fact that reduction of $CD8^+$ T cell apoptosis was not completely abrogated in RABV infected B7-$H1^{-/-}$ mice, may suggest that other pro-apoptotic factors were still expressed by B7-$H1^{-/-}$ infected neurons. The remaining $CD8^+$ T cells death could be the result of the expression of B7-DC the second receptor for PD-1, which expression was increased in neuronal cultures by RABV infection (**Figure 1 D**). Since B7-H1 is expressed by inflammatory cells ((11)and this manuscript) killing of $CD8^+$ T cells may also result of B7-H1 positive microglia and macrophages. Killing of $CD8^+$ T cells would thus be expected to occur in any NS infection in which interferon is produced, microglia is activated and macrophages infiltrate the NS. However, in such an infection model (West Nile infection) we did not observed any decrease in the number of migratory T cells (45). Thus it is unlikely that B7-H1 expressed by inflammatory cells is a major pathway to promote migratory T cell death in the infected NS.

Our findings are in good accordance with recent observations demonstrating that absence of B7-H1 leads to a more efficient elimination of adenovirus in mice (46) and that in human rhinovirus infection, the B7-H1/PD-1 pathway triggers a hindered immune response in the respiratory tract (23). They are also reminiscent of what has been observed in Schistosomia where infected macrophages up-regulate B7-H1 molecules thereby exhausting the host immune response (47). Very recently, PD-1 on T cells has been attributed to an exhausted phenotype of antigen-specific CD8 T cells, a phenomenon relevant in chronic infections with immuno-evasive viruses such as chronic lympho-chorio-meningitis virus, LCMV, (19), human immunodeficiency virus HIV (48, 49) and hepatitis C virus HCV (50, 51). But, our results also stress a specific and important aspect of RABV infection, its “organ-specificity”. Here, the B7-H1/PD1-pathway is specifically manipulated upon infection in the NS.

Expression of B7-H1 is modulated in this organ as well as B7-H1 induced changes in CD4/CD8 ratio in the NS. This takes place despite the fact that no change in the CD4/CD8 ratio occurred in the periphery and despite the fact that WT mice as well as B7-H1$^{-/-}$ mice develop similar RABV specific serum antibodies (data not shown), strongly suggesting that mounting of primary immune response against RABV was not altered by the absence of B7-H1. We can conclude that it is the specific B7-H1 over-expression in the RABV infected NS which contributes to the immunoevasiveness of the virus. However, among neuronotropic viruses, up-regulation of B7-H1 could not be shared by every virus since, as reported here, HSV-1 did not alter B7-H1 expression and only partially counteracts and escapes the host immune responses (7).

We observed that mice lacking TLR3 showed a reduced B7-H1 expression, suggesting that TLR3 signaling was involved in B7-H1 regulation. Since TLR3$^{-/-}$ mice develop a less severe form of RABV it can be hypothesized that TLR3 signaling pathway facilitates the immunoevasion. If this is the case, it will be reminiscent of the finding that in tumor cells, TLR4 signaling enhances immune suppression *in vitro* and that converse blockade of TLR4 prolongs the survival of mice grafted with tumor (52). Involvement of TLR signaling in induced B7-H1 expression has been observed in tumor cells where ligation of TLR2, 4 and 9 with agonists (PGN, LPS and ODN, respectively) induced B7-H1 expression (52,53). We recently established that human neurons express TLR3 and can mount a chemo-attractive, inflammatory and antiviral-including IFN-β responses after RABV infection. TLR3 expression was found to be enhanced by RABV infection in human neurons in cultures as well as in autopsied rabies cases (36, 54). Whether TLR3 signalling is also involved in B7-H1 deserves further investigation. Nevertheless, since signalisation through TLRs such as TLR3

leads to the mounting of an interferon response, IFN response may be one arm of the TLR3 mediated regulation of B7-H1.

Both type I and II interferons (IFN-β and γ) have been described to up-regulate B7-H1 transcripts in human DCs and monocytes (12). Interferon regulatory factor 1 (IRF1) is a crucial factor in the IFN-γ induced upregulation of B7-H1(55). Our results indicate that IFN-β and γ also control B7-H1 expression in human neurons and astrocytes as well as in mouse hippocampal neuronal cultures. In the course of RABV infection, IFN-β production by the infected NS precedes the onset of B7-H1 transcription which is virtually absent in non-infected NS. Severely impaired IFN-β production (as observed in RABV infected TLR3$^{-/-}$ mice) is associated with a decrease in B7-H1 transcription. Therefore, B7-H1 up-regulation in the NS occurs as a response or at least requires the presence of a specific "inflammatory" or cytokine milieu. The fact that HSV-1 does not trigger B7-H1 expression in HSV-1 infected neurons is fully consistent with the contribution that IFN-β exerts in the regulation of B7-H1 transcription, since HSV-1 strictly inhibits host IFN response (36, 56). It is surprising that B7-H1 expression in TLR3$^{-/-}$ brains was still reduced despite the production of large amounts of IFN-γ transcripts in these tissues. This may indicate that – at least *in vivo* - B7-H1 expression requires a production of IFN-β and γ above a certain threshold and/or that synergetic effects between the two cytokines are required.

In any case, these observations suggest that B7-H1 up-regulation in the NS occurs as a response to or in the presence of a specific "inflammatory" cytokine milieu (11). In the instance of autoimmune NS inflammation, expression of B7-H1 is localized within areas of strongest inflammation and is considered to act as a "negative" regulatory feedback loop for keeping the "anti-inflammatory milieu" in the NS (4). Such a tissue tolerance function of B7-H1 has similarly been postulated in other parenchymateous organs, as recently shown for the

pancreas in a disease model of autoimmune diabetes (9, 10). While the inhibitory function of tissue related B7-H1 is beneficial in the instance of (autoimmune) inflammatory aggression, it has opposite effects in the case of viral infection: here, the virus diverts a feed back loop to its own strategy. In the case of RABV, a pathogen well-adapted to the NS, we propose that B7-H1 acts as a viral target for immune evasion.

Our data support a sequential scheme of events after NS infection by RABV contributing to RABV immunoevasion. Early in NS infection by RABV, NS cells mount an innate immune response including TLR3 signalling and IFN-β production leading to B7-H1 expression. Infected neurons which express TLR3 can directly contribute to the IFN-β production. B7-H1 protein subsequently reaches the cell surface of the infected neurons, where it could interact with its main receptor PD-1 known to be expressed by T as well as B cells. Interaction of B7-H1 with PD-1 would then trigger the exhaustion of $CD8^+$ T cells (e.g. reducing cell expansion or promoting active elimination) and thus favour the viral invasion of the NS. This pathway appears of crucial importance to ensure the progression of the disease in the NS since mice eliminate much more efficiently the invading virus when it is abrogated.

Taken together, our data provide evidence for an important role of the B7-H1/PD-1 pathway in some neurotropic infections. The demonstration of neuronal expression of B7-H1 after a RABV infection and the fact that mice lacking B7-H1 have a significant survival advantage, clearly advocate the notion that B7-H1 is critically involved in the strategies employed by RABV to escape the host immune response. Interference affecting the B7-H1/PD-1 interactions might then be envisioned as a possible therapeutic approach to strengthen and expand actual post exposure treatment of human rabies.

Acknowledgments : We thank Pascal Roux for confocal microscopy, Anke Bauer for editing the manuscript, and Viviane Balloy and Mustapha Si-Tahar for the TLR3 mice breeding .

Legends

Figure 1. B7-H1 is expressed in human neural cells upon RABV infection or after IFN-β or γ treatment but not in cell lacking IFN-β. NT2-N, NT2-N/A or SKNSH were infected with RABV or treated with rIFN-β ,-γ or TNF–α. *B7-H1*, *B7-DC, CD80, CD86*, *IFN-β* expression and RABV infection was monitored by real time PCR. **A**) Kinetic of RABV infection (grey) and *B7-H1* transcripts (black) in NT2-N. Right panel B7-H1 transcripts in 24h HSV-1 infected NT2-N. Infection was monitored by RT PCR in RABV and HSV-1 infected cells by detecting RABV N protein or UL54 for HSV-1. 18S was used as a house-keeping gene. **B**) Surface expression of B7-H1 by cytofluorimetry in 24h-RABV infected SK-N-SH (bold) compared to non infected (solid) and irrelevant staining (dashed). Specific index of fluorescence was of 3. More than 88% of the SK-N-SH were infected. **C**) Relative gene expression of *B7-H1, B7-DC, CD80* and *CD86* were compared by real time PCR in non infected NT2-N cells (white) and in 24h RABV (dark) or HSV-1 (grey) infected NT2-N. 18S was used as a reporter gene. *CD200R* was used as a negative control (7). **D**) Effect of a 24h-treatment of rTNF–α (1.25ng), 500 U of rIFN–γ and IFN-β (1000 IU) on the *B7-H1* (black*)* and *B7-DC* (grey) transcription by non-infected NT2-N/A. **E**) Viral load (N protein transcripts), B7-H1, IFN-β and γ transcription were compared in SK-N-SH and in SK-N-SH-CP, a variant of SK-N-SH naturally disabled for IFNs were measured by real time PCR two days after infection. Data are presented as relative fold increase compared to non infected conditions.

Figure 2. Hippocampal cultures express B7H1 after incubation with IFN-γ and IFN-β.

5-7 days mouse foetal hippocampal cultures were either non-treated (NT) or treated with 500U/ml of IFN-γ or with 1000U/ml of IFN–β for 48h. B7-H1 (red) and neurofilament MAP-

2 (green) expressions were detected by immunocytochemistry. Nuclei are stained blue (DAPI). Bar represents 100µm.

Figure 3. Expression of *B7-H1* gene and protein in the mouse NS in the course of RABV infection. A) Expression of *B7-H1* (solid line) and *RABV N* (dotted line) transcripts were analyzed in non-infected (day 0) and day 5 and 10 RABV-infected spinal cord and brain by real time PCR. Results are given as mean +/- SD of relative fold increase of transcripts detected in samples of 2 or 3 mice. In this experiment, a gene (Insulin Like Growth factor) which expression was barely not modified by RABV infection had the following relative fold increases in the spinal cord : x1 at day 0; x2 at day 5, x1 at day 7 and in the brain : x1 at day 0 and 5, x1.7 at day 7. **B)** Immunohistochemistry was performed in day7 brain section. B7-H1 (red) was expressed by non-infected cells and by infected (green) neurons (arrows). 70% of infected neurons were B7-H1 positive. **C)** Orthogonal confocal microcopy analysis showed that B7-H1 accumulated in the cytoplasma of infected neurons. Bars represent 10 µm.

Figure 4. RABV infection triggers the expression of IFN-β and -γ in the mouse spinal cord and brain. A) Mice were injected with RABV in the hindlimbs and perfused. Spinal cord and brain were removed and subjected to transcriptional analysis. Transcription of *IFN–β* (black squares) and *IFN-γ* (white circles) were analyzed by real time PCR in non-infected (day 0) and RABV-infected spinal cord and brain at day 5 and 7 after infection. Results are given as mean of relative fold increase of transcripts detected in NS specimen of 2 or 3 mice with SD. **B**) $TLR3^{-/-}$ and C57Bl6 (WT) mice were infected with RABV. Transcription of *B7-H1, IFN-β* and *IFN-γ* were analysed by real time PCR in the brains of RABV infected $TLR3^{-/-}$ (black histograms) and WT mice (grey histograms) at day 5 and 7 post infection. 3 mice of each group were analysed for each time point. SD is indicated. *

indicates that levels of transcription are significantly different in TLR3$^{-/-}$ and WT brains (students T-test, $p<0.005$). Three separate experiments were performed.

Figure 5. Mice are protected against rabies in the absence of a functional *B7-H1* gene. Comparison of RABV infection in B7-H1$^{-/-}$ and C57Bl6 (WT) mice. **A**) Cumulative clinical symptoms in B7-H1$^{-/-}$ mice (black squares) compared to WT (white circles) after injection of a virus dose 50. **B)** Mortality after injection of virus dose 100 and 50 (n=8 mice each). **C**) Viral load (N protein transcripts) was measured at days 5 and 10 in the brain stem of B7-H1$^{-/-}$ and WT mice (virus dose 50; two mice each). Two separate experiments were performed.

Figure 6. In the absence of B7-H1 the characteristic exhaustion of migratory CD3$^+$ T cells into the NS of RABV infected mice did not occur. Phenotyping of splenocytes or mononuclear cells infiltrating the NS of WT or B7-H1$^{-/-}$ mice were analyzed by cytofluorimetry on days 5 and 10 post infection. **A)** Kinetic of CD3$^+$ T cell percentages among mononuclear cells invading the NS of B7-H1$^{-/-}$ (black) or WT mice (grey). **B**) Percentage at day 10 of CD4$^+$ and CD8$^+$ T cells among the migratory CD3$^+$ T cells in the NS of B7-H1$^{-/-}$ (black) and WT (grey) mice. * different at $p<0.0005$. **C**) Dot plot analysis of CD8$^+$ T cells among migratory CD3$^+$ T cells in the NS of B7-H1$^{-/-}$ and WT mice 10 days post infection. 20% and 3% represent the % of CD8$^+$ T cells in NS of B7-H1$^{-/-}$ and WT mice respectively, whereas 72% and 37% represent the % of infiltrating CD3$^+$T cells in B7-H1$^{-/-}$ and WT mice, respectively. **D**) CD4/CD8 ratio among migratory cells into the NS of B7-H1$^{-/-}$ and WT mice. **E)** Apoptosis of migratory CD8 + T cells was decreased in the absence of B7-H1 expression (B7-H1$^{-/-}$mice). Experiments were performed twice with 2-3 mice for each time point and condition.

References

1. Jackson, A. C. 2002. Update on rabies. Curr. Opin. Neurol. 15:327-331.
2. Warrell, M. J., and D. A. Warrell. 2004. Rabies and other lyssavirus diseases. Lancet 363:959-969.
3. Willoughby, R. E., Jr., K. S. Tieves, G. M. Hoffman, N. S. Ghanayem, C. M. Amlie-Lefond, M. J. Schwabe, M. J. Chusid, and C. E. Rupprecht. 2005. Survival after treatment of rabies with induction of coma. N. Engl. J. Med. 352:2508-2514.
4. Lafon, M. 2005. Modulation of the immune response in the nervous system by rabies virus. Curr. Top. Microbiol. Immunol. 289:239-258.
5. Baloul, L., and M. Lafon. 2003. Apoptosis and rabies virus neuroinvasion. Biochimie 85:777-788.
6. Baloul, L., S. Camelo, and M. Lafon. 2004. Up-regulation of Fas ligand (FasL) in the central nervous system: a mechanism of immune evasion by rabies virus. J. Neurovirol. 10:372-382.
7. Lafon, M., C. Prehaud, F. Megret, M. Lafage, G. Mouillot, M. Roa, P. Moreau, N. Rouas-Freiss, and E. D. Carosella. 2005. Modulation of HLA-G expression in human neural cells after neurotropic viral infections. J. Virol. 79:15226-15237.
8. Okazaki, T., and T. Honjo. 2006. Rejuvenating exhausted T cells during chronic viral infection. Cell 124:459-461.
9. Martin-Orozco, N., and C. Dong. 2006. New battlefields for costimulation. J. Exp. Med. 203:817-820.
10. Keir, M. E., Y. E. Latchman, G. J. Freeman, and A. H. Sharpe. 2005. Programmed death-1 (PD-1):PD-ligand 1 interactions inhibit TCR-mediated positive selection of thymocytes. J. Immunol. 175:7372-7379.

11. Magnus, T., B. Schreiner, T. Korn, C. Jack, H. Guo, J. Antel, I. Ifergan, L. Chen, F. Bischof, A. Bar-Or, and H. Wiendl. 2005. Microglial expression of the B7 family member B7 homolog 1 confers strong immune inhibition: implications for immune responses and autoimmunity in the CNS. J. Neurosci. 25:2537-2546.

12. Schreiner, B., M. Mitsdoerffer, B. C. Kieseier, L. Chen, H. P. Hartung, M. Weller, and H. Wiendl. 2004. Interferon-beta enhances monocyte and dendritic cell expression of B7-H1 (PD-L1), a strong inhibitor of autologous T-cell activation: relevance for the immune modulatory effect in multiple sclerosis. J. Neuroimmunol. 155:172-182.

13. Wang, L., R. Han, and W. W. Hancock. 2007. Programmed cell death 1 (PD-1) and its ligand PD-L1 are required for allograft tolerance. Eur. J. Immunol. 37:2983-2990.

14. Dong, H., G. Zhu, K. Tamada, and L. Chen. 1999. B7-H1, a third member of the B7 family, co-stimulates T-cell proliferation and interleukin-10 secretion. Nat. Med. 5:1365-1369.

15. Eppihimer, M. J., J. Gunn, G. J. Freeman, E. A. Greenfield, T. Chernova, J. Erickson, and J. P. Leonard. 2002. Expression and regulation of the PD-L1 immunoinhibitory molecule on microvascular endothelial cells. Microcirculation 9:133-145.

16. Latchman, Y., C. R. Wood, T. Chernova, D. Chaudhary, M. Borde, I. Chernova, Y. Iwai, A. J. Long, J. A. Brown, R. Nunes, E. A. Greenfield, K. Bourque, V. A. Boussiotis, L. L. Carter, B. M. Carreno, N. Malenkovich, H. Nishimura, T. Okazaki, T. Honjo, A. H. Sharpe, and G. J. Freeman. 2001. PD-L2 is a second ligand for PD-1 and inhibits T cell activation. Nat. Immunol. 2:261-268.

17. Wiendl, H., M. Mitsdoerffer, D. Schneider, L. Chen, H. Lochmuller, A. Melms, and M. Weller. 2003. Human muscle cells express a B7-related molecule, B7-H1, with strong negative immune regulatory potential: a novel mechanism of counterbalancing the immune attack in idiopathic inflammatory myopathies. Faseb J. 17:1892-1894.

18. Wintterle, S., B. Schreiner, M. Mitsdoerffer, D. Schneider, L. Chen, R. Meyermann, M. Weller, and H. Wiendl. 2003. Expression of the B7-related molecule B7-H1 by glioma cells: a potential mechanism of immune paralysis. Cancer Res. 63:7462-7467.

19. Barber, D. L., E. J. Wherry, D. Masopust, B. Zhu, J. P. Allison, A. H. Sharpe, G. J. Freeman, and R. Ahmed. 2006. Restoring function in exhausted CD8 T cells during chronic viral infection. Nature 439:682-687.

20. Hori, J., M. Wang, M. Miyashita, K. Tanemoto, H. Takahashi, T. Takemori, K. Okumura, H. Yagita, and M. Azuma. 2006. B7-H1-induced apoptosis as a mechanism of immune privilege of corneal allografts. J. Immunol. 177:5928-5935.

21. Salama, A. D., T. Chitnis, J. Imitola, M. J. Ansari, H. Akiba, F. Tushima, M. Azuma, H. Yagita, M. H. Sayegh, and S. J. Khoury. 2003. Critical role of the programmed death-1 (PD-1) pathway in regulation of experimental autoimmune encephalomyelitis. J. Exp. Med. 198:71-78.

22. Dong, H., S. E. Strome, D. R. Salomao, H. Tamura, F. Hirano, D. B. Flies, P. C. Roche, J. Lu, G. Zhu, K. Tamada, V. A. Lennon, E. Celis, and L. Chen. 2002. Tumor-associated B7-H1 promotes T-cell apoptosis: a potential mechanism of immune evasion. Nat. Med. 8:793-800.

23. Kirchberger, S., O. Majdic, P. Steinberger, S. Bluml, K. Pfistershammer, G. Zlabinger, L. Deszcz, E. Kuechler, W. Knapp, and J. Stockl. 2005. Human rhinoviruses inhibit the accessory function of dendritic cells by inducing sialoadhesin and B7-H1 expression. J. Immunol. 175:1145-1152.

24. Rouse, B. T., and D. Masopust. 2006. Waking up T cells to counteract chronic infections. Trends Immunol. 27:205-207.

25. Zhu, B., I. Guleria, A. Khosroshahi, T. Chitnis, J. Imitola, M. Azuma, H. Yagita, M. H. Sayegh, and S. J. Khoury. 2006. Differential Role of Programmed Death-1 Ligand

and Programmed Death-2 Ligand in Regulating the Susceptibility and Chronic Progression of Experimental Autoimmune Encephalomyelitis. J. Immunol. 176:3480-3489.

26. Latchman, Y. E., S. C. Liang, Y. Wu, T. Chernova, R. A. Sobel, M. Klemm, V. K. Kuchroo, G. J. Freeman, and A. H. Sharpe. 2004. PD-L1-deficient mice show that PD-L1 on T cells, antigen-presenting cells, and host tissues negatively regulates T cells. Proc. Natl. Acad. Sci. U S A 101:10691-10696.

27. Camelo, S., M. Lafage, and M. Lafon. 2000. Absence of the p55 Kd TNF-alpha receptor promotes survival in rabies virus acute encephalitis. J. Neurovirol. 6:507-518.

28. Thoulouze, M. I., M. Lafage, J. A. Montano-Hirose, and M. Lafon. 1997. Rabies virus infects mouse and human lymphocytes and induces apoptosis. J. Virol. 71:7372-7380.

29. Smith, K. O. 1964. Relationship between the Envelope and the Infectivity of Herpes Simplex Virus. Proc. Soc. Exp. Biol. Med. 115:814-816.

30. Dong, H., G. Zhu, K. Tamada, D. B. Flies, J. M. van Deursen, and L. Chen. 2004. B7-H1 determines accumulation and deletion of intrahepatic CD8(+) T lymphocytes. Immunity 20:327-336.

31. Alexopoulou, L., A. C. Holt, R. Medzhitov, and R. A. Flavell. 2001. Recognition of double-stranded RNA and activation of NF-kappaB by Toll-like receptor 3. Nature 413:732-738.

32. Pleasure, S. J., C. Page, and V. M. Lee. 1992. Pure, postmitotic, polarized human neurons derived from NTera 2 cells provide a system for expressing exogenous proteins in terminally differentiated neurons. J. Neurosci. 12:1802-1815.

33. Sandhu, J. K., M. Sikorska, and P. R. Walker. 2002. Characterization of astrocytes derived from human NTera-2/D1 embryonal carcinoma cells. J. Neurosci. Res. 68:604-614.

34. Cheung, W. M., W. Y. Fu, W. S. Hui, and N. Y. Ip. 1999. Production of human CNS neurons from embryonal carcinoma cells using a cell aggregation method. Biotechniques 26:946-948.

35. Paquet-Durand, F., S. Tan, and G. Bicker. 2003. Turning teratocarcinoma cells into neurons: rapid differentiation of NT-2 cells in floating spheres. Brain Res. Dev. Brain Res. 142:161-167.

36. Prehaud, C., F. Megret, M. Lafage, and M. Lafon. 2005. Virus infection switches TLR-3-positive human neurons to become strong producers of beta interferon. J. Virol. 79:12893-12904.

37. Galelli, A., L. Baloul, and M. Lafon. 2000. Abortive rabies virus central nervous infection is controlled by T lymphocyte local recruitment and induction of apoptosis. J. Neurovirol. 6:359-372.

38. Kishimoto, H., C. D. Surh, and J. Sprent. 1995. Upregulation of surface markers on dying thymocytes. J. Exp. Med. 181:649-655.

39. Thoulouze, M. I., M. Lafage, V. J. Yuste, L. Baloul, L. Edelman, G. Kroemer, N. Israel, S. A. Susin, and M. Lafon. 2003. High level of Bcl-2 counteracts apoptosis mediated by a live rabies virus vaccine strain and induces long-term infection. Virology 314:549-561.

40. Trojanowski, J. Q., S. R. Kleppner, R. S. Hartley, M. Miyazono, N. W. Fraser, S. Kesari, and V. M. Lee. 1997. Transfectable and transplantable postmitotic human neurons: a potential "platform" for gene therapy of nervous system diseases. Exp. Neurol. 144:92-97.

41. Kleppner, S. R., K. A. Robinson, J. Q. Trojanowski, and V. M. Lee. 1995. Transplanted human neurons derived from a teratocarcinoma cell line (NTera-2)

mature, integrate, and survive for over 1 year in the nude mouse brain. J. Comp. Neurol. 357:618-632.

42. Murphy, F. A. 1977. Rabies pathogenesis. Arch. Virol. 54:279-297.

43. Jackson, A. C. 2003. Rabies virus infection: an update. J. Neurovirol. 9:253-258.

44. Lafon, M. 2004. Subversive neuroinvasive strategy of rabies virus. Arch. Virol. Suppl:149-159.

45. Brehin, A.-C., J. Mouries, M.-P. Frenkiel, G. Dadaglio, P. Despres, M. Lafon, and T. Couderc. 2008. Dynamics of immune cell recruitment during West Nile encephalitis and identification of a new $CD19^{+}$ $B220^{-}$ $BST\text{-}2^{+}$ leukocyte population. J. Immunol. 180 : 6760-6767.

46. Iwai, Y., S. Terawaki, M. Ikegawa, T. Okazaki, and T. Honjo. 2003. PD-1 inhibits antiviral immunity at the effector phase in the liver. J. Exp. Med. 198:39-50.

47. Smith, P., C. M. Walsh, N. E. Mangan, R. E. Fallon, J. R. Sayers, A. N. McKenzie, and P. G. Fallon. 2004. Schistosoma mansoni worms induce anergy of T cells via selective up-regulation of programmed death ligand 1 on macrophages. J. Immunol. 173:1240-1248.

48. Trautmann, L., L. Janbazian, N. Chomont, E. A. Said, S. Gimmig, B. Bessette, M. R. Boulassel, E. Delwart, H. Sepulveda, R. S. Balderas, J. P. Routy, E. K. Haddad, and R. P. Sekaly. 2006. Upregulation of PD-1 expression on HIV-specific CD8+ T cells leads to reversible immune dysfunction. Nat. Med. 12:1198-1202.

49. Day, C. L., D. E. Kaufmann, P. Kiepiela, J. A. Brown, E. S. Moodley, S. Reddy, E. W. Mackey, J. D. Miller, A. J. Leslie, C. DePierres, Z. Mncube, J. Duraiswamy, B. Zhu, Q. Eichbaum, M. Altfeld, E. J. Wherry, H. M. Coovadia, P. J. Goulder, P. Klenerman, R. Ahmed, G. J. Freeman, and B. D. Walker. 2006. PD-1 expression on HIV-specific

T cells is associated with T-cell exhaustion and disease progression. Nature 443:350-354.

50. Urbani, S., B. Amadei, D. Tola, M. Massari, S. Schivazappa, G. Missale, and C. Ferrari. 2006. PD-1 expression in acute hepatitis C virus (HCV) infection is associated with HCV-specific CD8 exhaustion. J. Virol. 80:11398-11403.

51. Grakoui, A., E. John Wherry, H. L. Hanson, C. Walker, and R. Ahmed. 2006. Turning on the off switch: regulation of anti-viral T cell responses in the liver by the PD-1/PD-L1 pathway. J. Hepatol. 45:468-472.

52. Huang, B., J. Zhao, H. Li, K. L. He, Y. Chen, S. H. Chen, L. Mayer, J. C. Unkeless, and H. Xiong. 2005. Toll-like receptors on tumor cells facilitate evasion of immune surveillance. Cancer Res. 65:5009-5014.

53. Liu, J., A. Hamrouni, D. Wolowiec, V. Coiteux, K. Kuliczkowski, D. Hetuin, A. Saudemont, and B. Quesnel. 2007. Plasma cells from multiple myeloma patients express B7-H1 (PD-L1) and increase expression following stimulation with IFN-{gamma} and TLR ligands via a MyD88-, TRAF6-, and MEK-dependent pathway. Blood. 110:296-304.

54. Jackson, A. C., J. P. Rossiter, and M. Lafon. 2006. Expression of Toll-like receptor 3 in the human cerebellar cortex in rabies, herpes simplex encephalitis, and other neurological diseases. J. Neurovirol. 12:229-234.

55. Lee, S. J., B. C. Jang, S. W. Lee, Y. I. Yang, S. I. Suh, Y. M. Park, S. Oh, J. G. Shin, S. Yao, L. Chen, and I. H. Choi. 2006. Interferon regulatory factor-1 is prerequisite to the constitutive expression and IFN-gamma-induced upregulation of B7-H1 (CD274). FEBS Lett. 580:755-762.

56. Jun, H., S. K. Seo, H. Y. Jeong, H. M. Seo, G. Zhu, L. Chen, and I. H. Choi. 2005. B7-H1 (CD274) inhibits the development of herpetic stromal keratitis (HSK). FEBS Lett. 579:6259-6264.

A

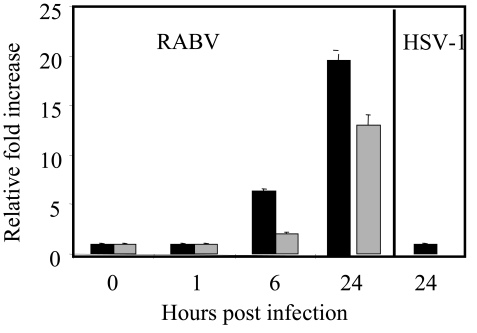

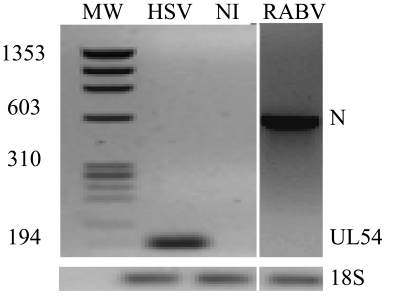

B

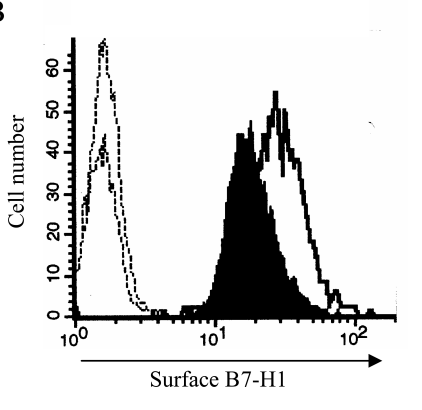

C

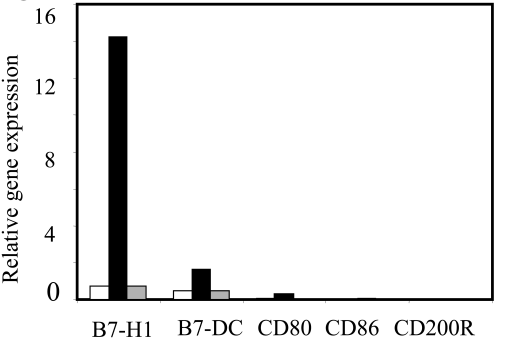

D

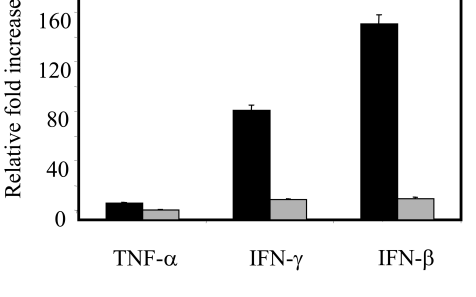

E

	SK-N-SH	SK-N-SH-CP
RABV	3 000 061	3 805 765
B7-H1	11	1
IFN-β	7	1
IFN-γ	2	2

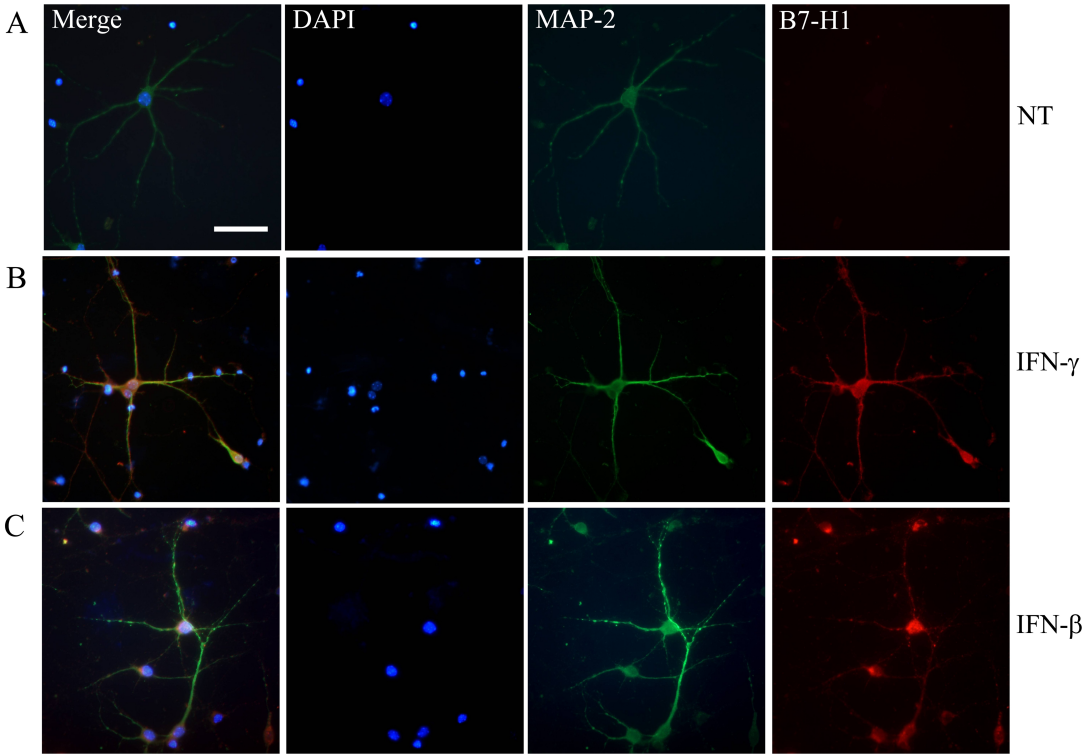
A
Merge
DAPI
MAP-2
B7-H1
NT
B
IFN-γ
C
IFN-β

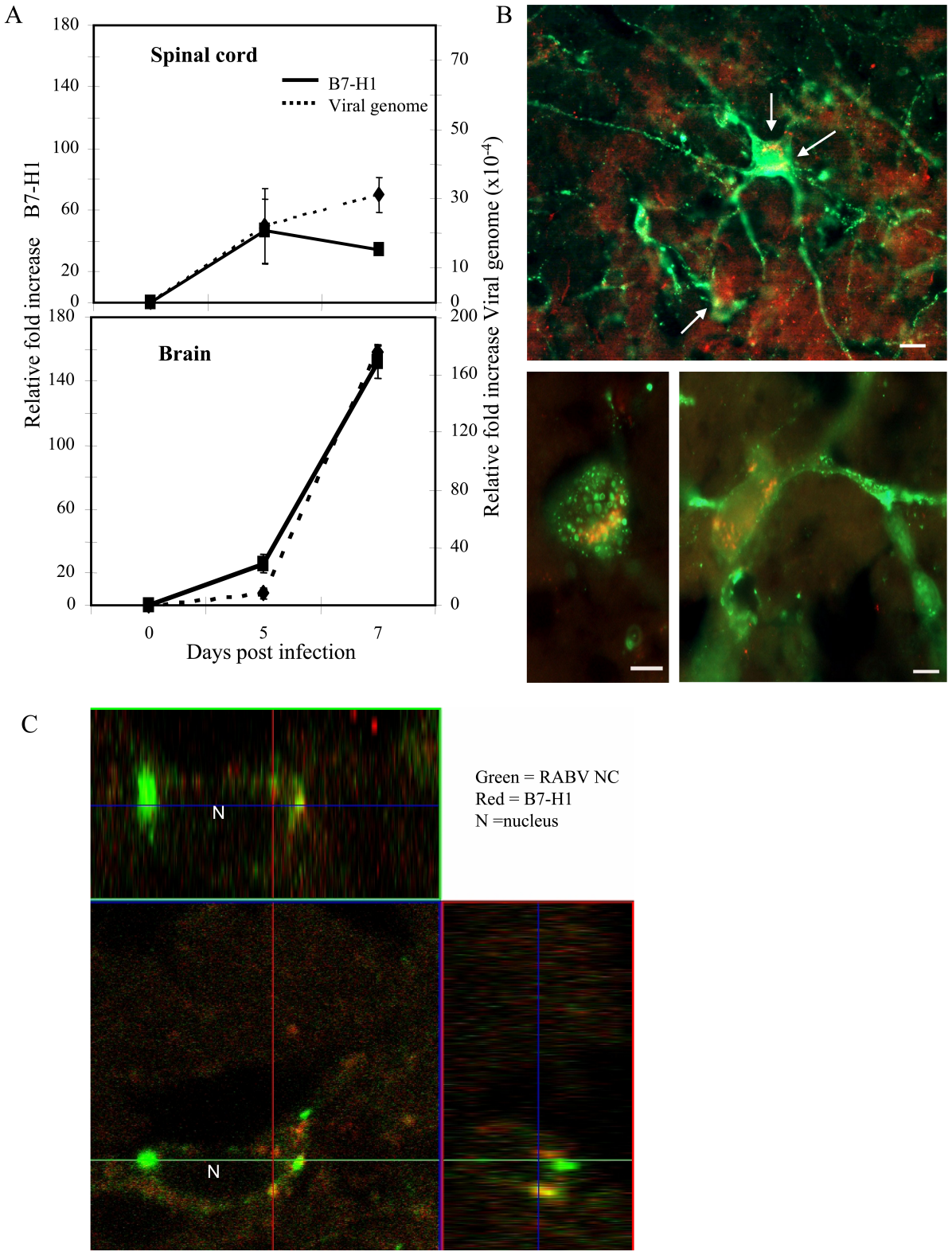
A
Spinal cord
B7-H1
Viral genome
Brain
Relative fold increase B7-H1
Relative fold increase Viral genome (x10-4)
Days post infection
0
5
7
B
C
N
N
Green = RABV NC
Red = B7-H1
N =nucleus

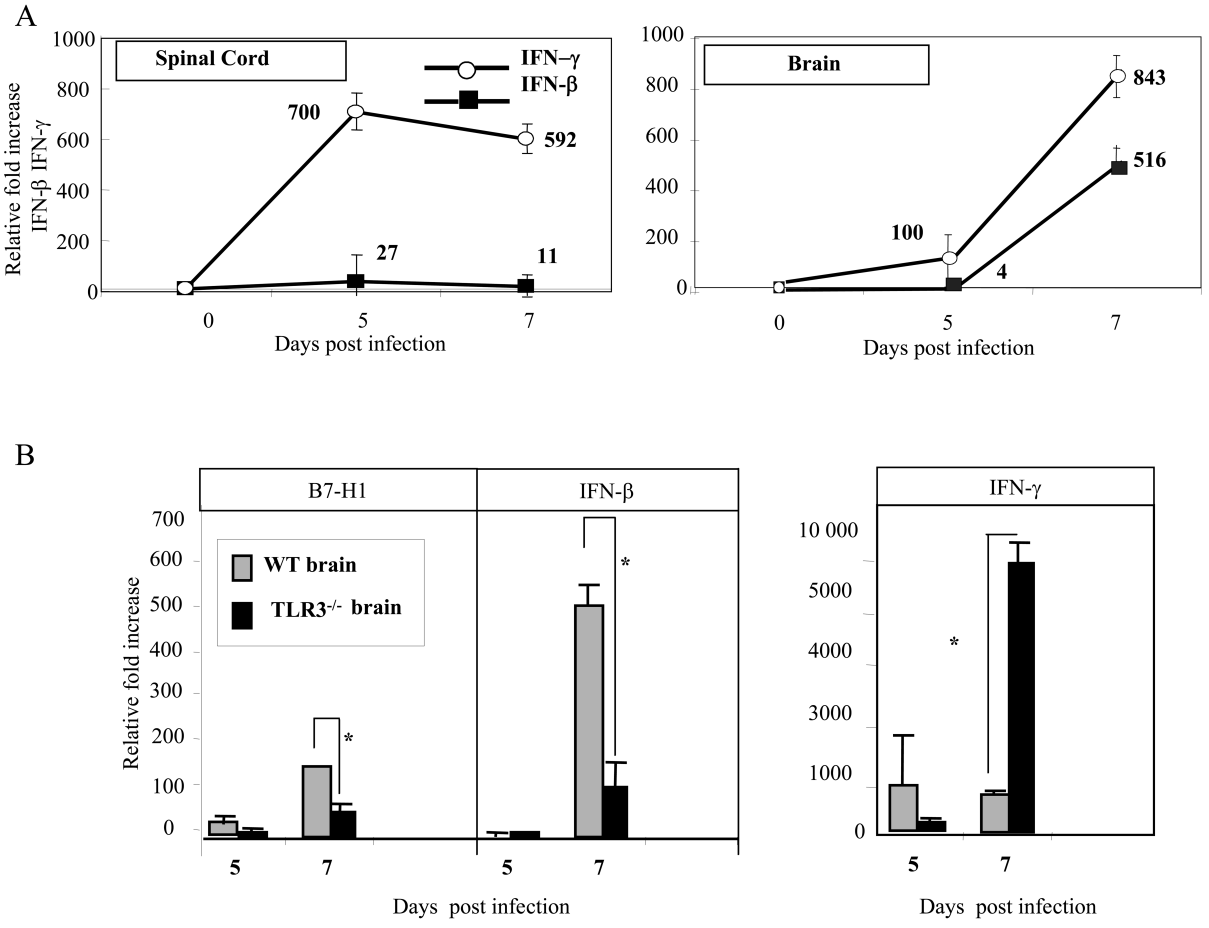
A
Spinal Cord
IFN–γ
IFN-β
Relative fold increase
IFN-β IFN-γ
1000
800
600
400
200
0
700
592
27
11
0
5
7
Days post infection
Brain
843
516
100
4
B
B7-H1
IFN-β
IFN-γ
WT brain
TLR3-/- brain
Relative fold increase
700
600
500
400
300
200
100
0
10 000
5000
4000
3000
1000
*
5
7
Days post infection

A

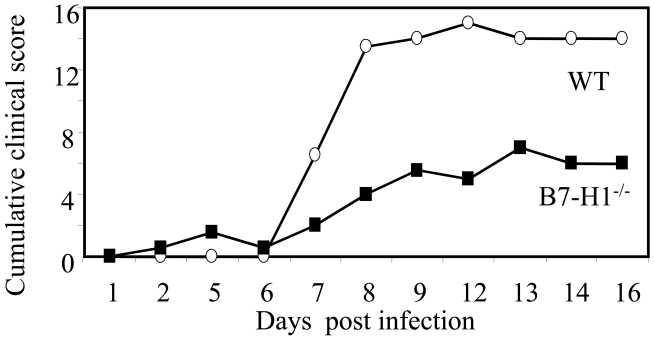

B

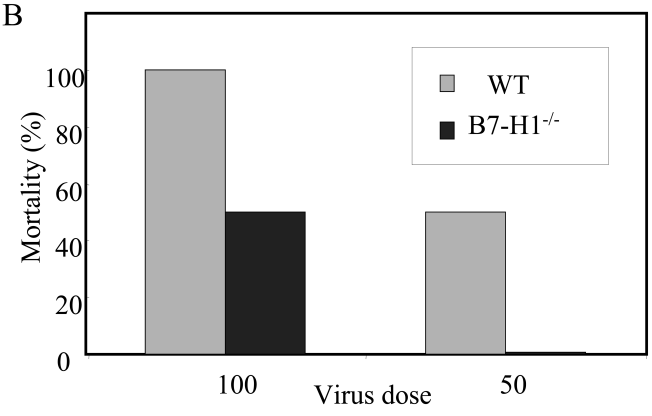

C

Infection	WT	B7-H1$^{-/-}$
Day 0	1	1
Day 5	3.200	83
Day 10	320.000	461

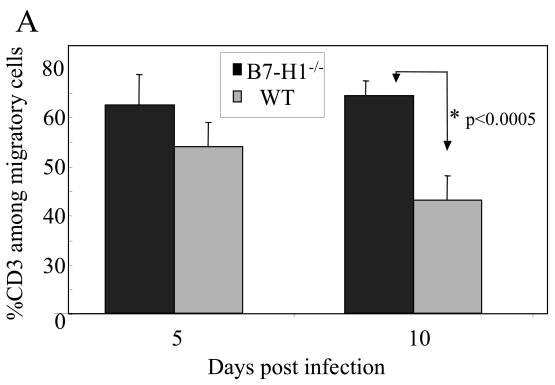

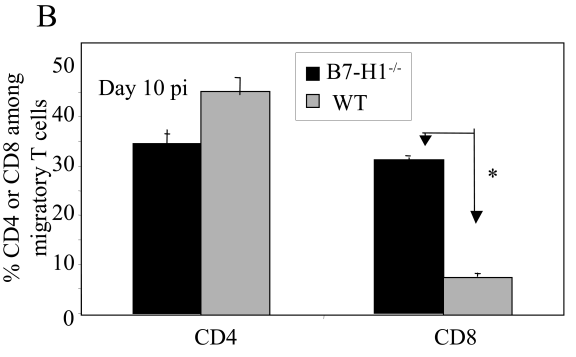

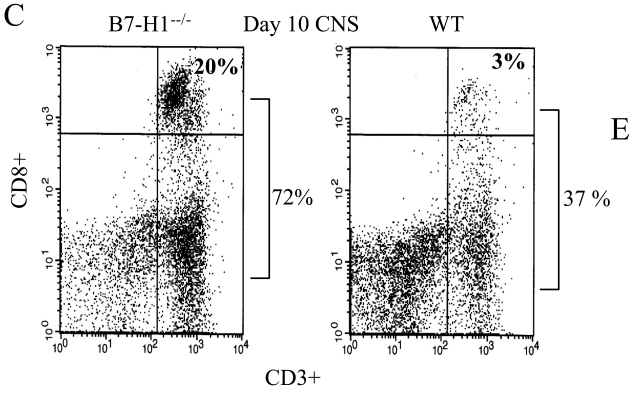

D

CD4/CD8	Day 5	Day 10
WT	2.9	5.8
B7-H1-/-	2.1	1.1